Constitutive Activation of the Shaker Kv Channel

Manana Sukhareva, David H. Hackos, and Kenton J. Swartz

Molecular Physiology and Biophysics Section, National Institute of Neurological Disorders and Stroke, National Institutes of Health, Bethesda, MD 20892

ABSTRACT In different types of K^+ channels the primary activation gate is thought to reside near the intracellular entrance to the ion conduction pore. In the Shaker Kv channel the gate is closed at negative membrane voltages, but can be opened with membrane depolarization. In a previous study of the S6 activation gate in Shaker (Hackos, D.H., T.H. Chang, and K.J. Swartz. 2002. *J. Gen. Physiol.* 119:521–532.), we found that mutation of Pro 475 to Asp results in a channel that displays a large macroscopic conductance at negative membrane voltages, with only small increases in conductance with membrane depolarization. In the present study we explore the mechanism underlying this constitutively conducting phenotype using both macroscopic and single-channel recordings, and probes that interact with the voltage sensors or the intracellular entrance to the ion conduction pore. Our results suggest that constitutive conduction results from a dramatic perturbation of the closed-open equilibrium, enabling opening of the activation gate without voltage-sensor activation. This mechanism is discussed in the context of allosteric models for activation of Kv channels and what is known about the structure of this critical region in K^+ channels.

KEY WORDS: voltage-dependent gating • hanatoxin • agitoxin • mutagenesis • potassium channel

INTRODUCTION

Voltage-gated K^+ (Kv) channels open and close in response to changes in membrane voltage, a property that underlies their role in electrical signaling throughout biology. These channels are tetramers, with each subunit containing six transmembrane segments, termed S1 through S6. The region of the protein that senses changes in membrane voltage is contained within the S1-S4 domain, with S4 containing the highest density of charged residues (Yellen, 1998; Li-Smerin et al., 2000a; Lu et al., 2001; Bezanilla, 2002; Gandhi and Isacoff, 2002; Jiang et al., 2003). The tetrameric arrangement of the S5 through S6 regions forms the ion-conduction pore, providing a pathway for ions to cross the membrane in the open state. In the closed state, ion permeation is minimized by an activation gate that is formed by the S6 segment at the intracellular entrance to the pore (Armstrong, 1969, 1971; Armstrong et and Hille, 1972; Holmgren et al., 1997; Liu et al., 1997; Holmgren et al., 1998; del Camino and Yellen, 2001; Zhou et al., 2001a; Hackos et al., 2002; Soler-Llavina et al., 2003) (Fig. 1 A). Structural studies on prokaryotic K^+ channels in conformations that can be equated with open and closed states further supports the notion of a gate at the intracellular pore entrance (Doyle et al., 1998; Roux et al., 2000; Zhou et al., 2001a; Jiang et al., 2002a,b, 2003). When opening, the inner helices that line the pore in these channels, equivalent to the S6 segment in Kv channels, have been proposed to bend at a conserved Gly residue (Fig. 1 B, pink shading), dramatically widening the intracellular entrance to the ion conduction pathway (Jiang et al., 2002b).

In the Shaker Kv channel, the S6 activation gate is closed at negative membrane voltages, but can be opened with membrane depolarization. A previous mutagenic scan of the S6 activation gate in Shaker identified several positions that are particularly sensitive to mutation (Hackos et al., 2002). For example, mutation of Pro 475 to Asp (Fig. 1 B, blue shading) results in a channel that displays a large macroscopic conductance at negative membrane voltages where the wild-type channel is normally closed. In contrast, mutation of Val 478 to Trp (Fig. 1 B, green shading) results in a channel that traffics to the plasma membrane, but does not conduct ions even though the voltage-sensors can translocate gating charge (Hackos et al., 2002). In the Shaker Kv channel, residues P475 and V478 are positioned within the region that displays pronounced changes in accessibility during opening (Liu et al., 1997; del Camino and Yellen, 2001), intracellular to the Gly residue (466) that has been proposed to function as a gating hinge. In this paper we examine three basic types of mechanisms that might explain the constitutively conducting phenotype that is observed in the P475D mutant channel. First, it is possible that the mutation effectively disrupts the structure of the S6 gate so that it no longer participates in gat-

Manana Sukhareva and David H. Hackos contributed equally to this paper.

Address correspondence to Kenton J. Swartz, Molecular Physiology and Biophysics Section, National Institute of Neurological Disorders and Stroke, National Institutes of Health, Building 36, Room 2C19, 36 Convent Drive, MSC 4066, Bethesda, MD 20892. Fax: (301) 435-5666; email: swartzk@ninds.nih.gov

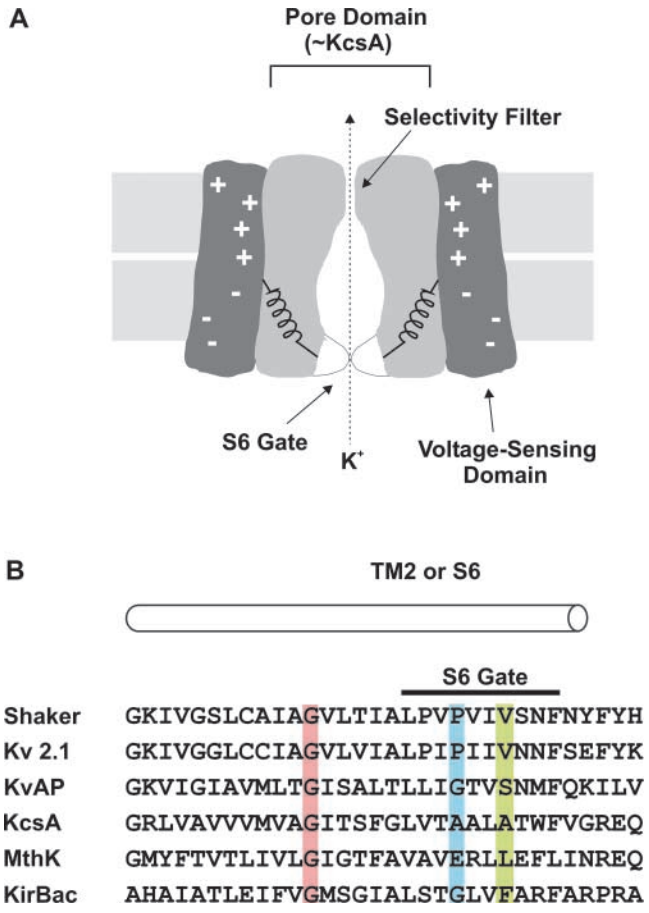

FIGURE 1. The intracellular gate region of K^+ channels. (A) Cartoon of a voltage-gated K^+ channel showing separate voltage-sensing and pore domains and an S6 activation gate toward the intracellular side of the pore. (B) Sequence alignment between Kv channels, KcsA, MthK and KirBac. Pink highlighting marks the conserved Gly residue that is proposed to serve as the gating hinge (Jiang et al., 2002a,b). Blue highlighting marks the position of P475 in Shaker, corresponding to P406 in Kv2.1, G229 in KvAP, A108 in KcsA, E92 in MthK, and G143 in KirBac. Green highlighting marks positions equivalent to V478 in Shaker, where Trp substitutions result in nonconducting channels (Hackos et al., 2002).

ing. A second possibility is that the mutation increases the conductance of the closed state (Soler-Llavina et al., 2003) without completely eliminating the ability of the S6 gate region to decrease the flow of K^+ ions in the closed state. Finally, it is possible that the mutation perturbs the closed to open equilibrium in a way that allows for opening of the activation gate without prior activation of the voltage sensors. We explore these possible mechanisms using both macroscopic and single-channel recordings, and probes that interact with the voltage sensors or the intracellular entrance to the ion conduction pore. Our results point to constitutive activation of the channel resulting from a dramatic perturbation of the closed to open equilibrium.

MATERIALS AND METHODS

Molecular Biology and Channel Expression

Experiments were performed using the Shaker H4 Kv channel (Kamb and et al., 1988) in pBlu-SK+ or the Kv2.1 (Frech et al., 1989) Δ7 channel in pBlu-SK−. Kv2.1Δ7 contains seven mutations in the S5-S6 linker (Aggarwal and MacKinnon, 1996; Li-Smerin and Swartz, 1998) that render the channel sensitive to the pore-blocking toxin Agitoxin-2, thus enabling the toxin to be used to subtract background conductances. Except for the experiment in Fig. 7, B and C, the Shaker Kv channel contains a deletion of residues 6–46 to remove fast N-type inactivation (Hoshi et al., 1990; Zagotta et al., 1990). Point mutations in Shaker and Kv2.1 were generated through sequential PCR and ligation into appropriately digested vectors. All mutations were verified using automated DNA sequencing. Shaker and Kv2.1 cDNA constructs were linearized with HindIII and NotI, respectively, and then transcribed using T7 RNA polymerase. *Xenopus laevis* oocytes were removed surgically and incubated with agitation for 1–1.5 h in a solution containing (in mM): 82.5 NaCl, 2.5 KCl, 1 $MgCl_2$, 5 HEPES, and 2 mg/ml collagenase (Worthington Biochemical Corp.), pH 7.6 with NaOH. Defolliculated oocytes were injected with cRNA and incubated at 17°C in a solution containing (in mM): 96 NaCl, 2 KCl, 1 $MgCl_2$, 1.8 $CaCl_2$, 5 HEPES, and 50 μg/ml gentamicin (Invitrogen/GIBCO BRL), pH 7.6 with NaOH until electrophysiological recording.

Electrophysiological Recording

Macroscopic ionic currents were recorded using two-electrode voltage clamp recording techniques between 1 and 5 d after cRNA injection using an OC-725C oocyte clamp (Warner Instruments). In most instances, oocytes were studied in a 160 μl recording chamber that was perfused with a solution containing (in mM): 50 RbCl, 50 NaCl, 1 $MgCl_2$, 0.3 $CaCl_2$, and 5 HEPES, pH 7.6 with NaOH. In several experiments, where noted, 50 mM KCl was used instead of RbCl. Data were filtered at 2 kHz (8-pole Bessel) and digitized at 10 kHz. Microelectrode resistances were between 0.2–1.2 MΩ when filled with 3 M KCl. Linear capacity, leak, and endogenous currents were subtracted after obtaining voltage-activation relations in the absence and presence of Agitoxin-2 (100 nM to 1 μM) (Garcia et al., 1994). Voltage-activation relations were fit with single Boltzmann functions according to:

$$G/G_{max} = (1 + e^{-zF(V - V_{50})/RT})^{-1}, \quad (1)$$

where G/G_{max} is obtained from normalized tail current amplitude, z is the equivalent charge, V50 is the half-activation voltage, F is Faraday's constant, R is the gas constant, and T is temperature in Kelvin.

Unitary currents were recorded in inside-out patches using a patch-clamp amplifier (Axopatch 200B). Data were filtered at 1 or 2 kHz (8-pole Bessel) and digitized at 20 kHz. Patch pipette resistance when filled with the recording solution was 10–15 MΩ. For the data presented in Fig. 8 the intracellular (bath) solution contained (in mM): 140 RbCl, 4 EGTA, 1 $CaCl_2$, 2 $MgCl_2$, 5 HEPES, pH 7.6, and the extracellular (pipette) solution contained (in mM): 140 RbCl, 1 $CaCl_2$, 2 $MgCl_2$, 5 HEPES, pH 7.6. For the data in Figs. 10 and 11, 140 mM KCl was used instead of RbCl for reasons described in the text, but otherwise the solutions were identical. Leak and capacitive currents were subtracted using null sweeps with no openings. All experiments were performed at room temperature (~22°C).

When the membrane of a cell expressing the wild-type Shaker Kv channel is held at negative voltages (e.g., −90 mV), the channel predominantly adopts a closed conformation. If the membrane is subsequently depolarized, the voltage sensors activate and the intracellular activation gate opens, allowing the channel to conduct K^+ ions. An illustration of this behavior for the wild-type Shaker Kv channel is shown in Fig. 2, A and B, where the channel was expressed in *Xenopus* oocytes and studied using two-electrode voltage clamp recording techniques with an external solutions containing 50 mM K^+ (internal K^+ is ∼100 mM). There is no detectable macroscopic K^+ current observed at the negative holding voltage (Fig. 2 A, arrow), but robust voltage-activated K^+ currents following depolarization above −50 mV. A strikingly different situation is seen for the mutation of Pro475 to Asp in the Shaker Kv channel where even at −150 mV there is a large standing conductance (Fig. 2 A, arrow), a phenomenon that we will refer to as a constitutive conductance. Although a large fraction of the conductance appears to be voltage independent, there are small and steeply voltage-dependent changes in macroscopic conductance that occur with membrane depolarization (Fig. 2, A and B), suggesting that some form of gating remains intact. Fitting of a single Boltzmann function to these voltage-dependent changes in conductance yields a midpoint (V_{50}) of −100 mV and a slope (z) of ∼3. Unless otherwise indicated, all of the current records presented here were obtained by subtracting endogenous and leak currents that remained after blocking the Shaker Kv channel with Agitoxin-2, a Kv channel-specific pore-blocking toxin (Garcia et al., 1994; Miller, 1995). Thus, we are confident that the large constitutive conductance is not due to leak or endogenous conductances, but arises from the expressed Shaker Kv channel.

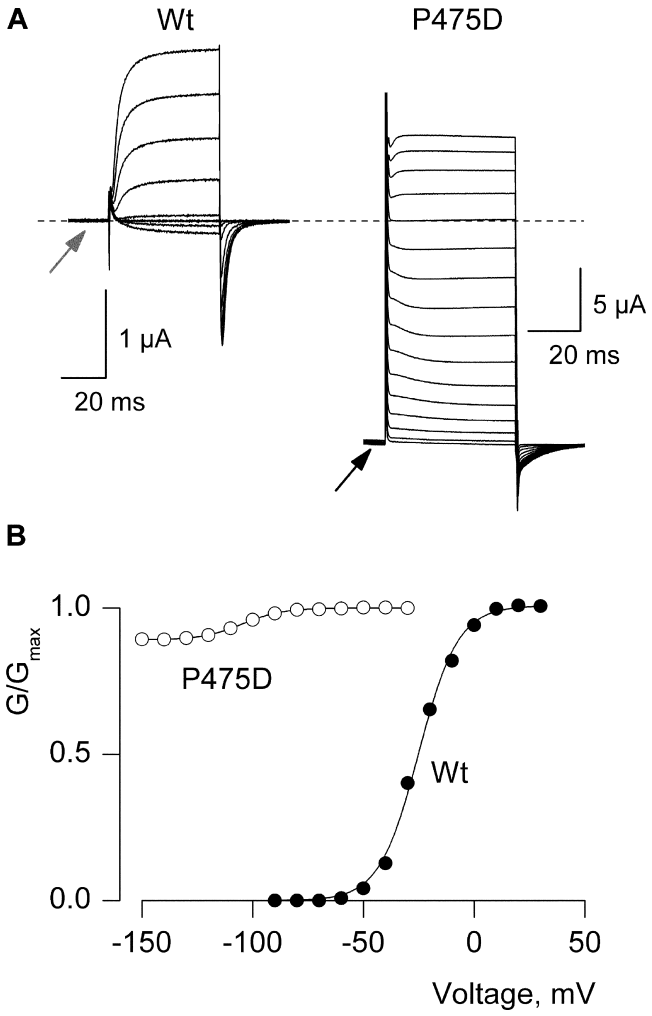

FIGURE 2. Constitutive conduction for the P475D mutant of the Shaker Kv channel. (A) Families of Agitoxin-sensitive ionic currents for oocytes expressing the wild-type or P475D mutant Shaker Kv channels. For wild-type, holding voltage was −90 mV, tail voltage was −60 mV, and depolarizations were from −60 to +20 mV in 10-mV steps. For P475D the holding voltage was −110 mV and membrane voltage was stepped to −150 mV for 200 ms before recording the traces shown. Tail voltage was −150 mV, and depolarizations were from −140 to +10 mV, in 10-mV increments. Charge carrier in the external solution was 50 mM K^+ and endogenous K^+ is ∼100 mM. Linear capacity and background conductances were identified and subtracted by blocking the Shaker channel with Agitoxin-2. Dashed line indicates the position of zero current. (B) Conductance (G)-voltage (V) relations for wild-type and P475D. Normalized tail current amplitudes are plotted versus the voltage of the preceding depolarization. Smooth curves are single Boltzmann fits to the data with parameters as follows: Wt, V_{50} = −25 mV, z = 3; P475D, V_{50} = −100 mV, z = 2.9.

Gating Properties of Different Substitutions at P475

To begin our studies of the mechanism underlying this constitutively conducting phenotype we explored the side-chain dependence of the phenotype by mutating P475 to all other amino acids and examining the gating behavior of each mutant. In each case we recorded macroscopic currents using a standard external solution containing 50 mM Rb^+.

As shown in Fig. 3, the constitutively conducting phenotype is not restricted to the Asp substitution, but is observed with other hydrophilic substitutions, including Gln, Asn, His, Lys, Arg, and Glu (Fig. 3, A and B; Table I). Interestingly, the degree of constitutive conduction is not fixed, but varies considerably for the different hydrophilic substitutions. For example, the fractional constitutive conductance (defined here as the limiting conductance at negative voltages divided by the maximal conductance at positive voltages) is ∼0.3 for P475Q, ∼0.05 for P475N, and ∼0.9 for P475D. In contrast to hydrophilic substitutions at P475, mutations to Trp, Tyr, Phe, Met, Cys, Ile, Val, Thr, Ser, and Gly result in channels that are similar to the wild-type in that they exhibit undetectable macroscopic current at

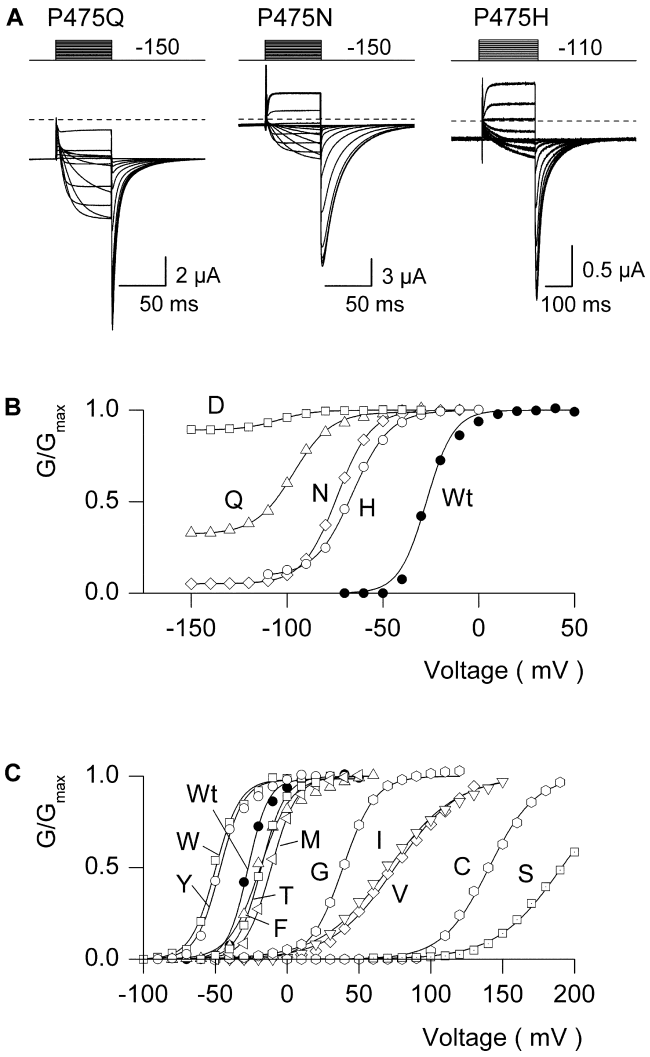

FIGURE 3. Gating properties for different substitutions at P475 in the Shaker Kv channel. (A) Families of ionic currents for three mutant Shaker channels. For P475Q and P475N, cells were held at −100 mV and stepped to −150 mV for 200 ms before the traces shown, tail voltage was −150 mV, and depolarizations were from −150 to −30 mV for Q and to −10 mV for N (each in 10-mV steps). For P475H, holding voltage was −110 mV, tail voltage was −110 mV, and depolarizations were from −110 to −10 mV (10-mV steps). Linear capacity and background conductances were identified and subtracted by blocking the Shaker channel with Agitoxin-2. Horizontal dashed lines correspond to the zero current level. (B) G-V relations for Wt and four P475 mutants displaying constitutive conduction. Normalized tail current amplitudes are plotted versus voltage of the preceding depolarization. For P475D the external solution contained 50 mM KCl and for all others 50 mM RbCl was used. Smooth curves are single Boltzmann fits to the data with parameters as follows: Wt, V_{50} = −27.3 mV, z = 3.6; P475D, V_{50} = −104 mV, z = 2.8; P475Q, V_{50} = −96.7 mV, z = 2.6; P475N, V_{50} = −73.9 mV, z = 2.9; P475H, V_{50} = −65.9 mV, z = 2.6. (C) G-V relations for Wt and 10 P475 mutants with undetectable constitutive conduction. Parameters for single Boltzmann fits are: P475W, V_{50} = −49.9 mV, z = 3.0; P475Y, V_{50} = −46.8 mV, z = 3.1; P475F, V_{50} = −19.0 mV, z = 2.4; P475T, V_{50} = −18.1 mV, z = 3.0; P475M: V_{50} = −11.1 mV, z = 2.8; P475G, V_{50} = +39 mV, z = 2.3; P475I, V_{50} = +71 mV, z = 1.1; P475V, V_{50} = +75 mV, z = 1.1; P475C, V_{50} = +141 mV, z = 1.6; P475S, V_{50} = +191 mV, z = 1.1.

TABLE I

Voltage Activation Relations for Shaker Kv Channels with Mutations at P475

Residue	V_{50}	z	*n*
	mV		
P (Wt)	−30.5 ± 0.6	3.8 ± 0.1	37
G	44.6 ± 1.3	2.2 ± 0.02	4
S	195.0 ± 5.7	1.2 ± 0.03	4
T	−15.0 ± 1.5	3.3 ± 0.08	8
Y	−48.3 ± 0.5	3.7 ± 0.1	10
V	64.8 ± 1.0	1.6 ± 0.08	6
I	63.9 ± 1.7	1.2 ± 0.04	5
M	−11.9 ± 0.2	2.8 ± 0.06	9
C	146 ± 3.0	1.3 ± 0.07	3
F	−21.6 ± 0.8	3.0 ± 0.09	10
W	−49.4 ± 1.8	4.0 ± 0.3	14
Q	−95.2 ± 1.0	2.6 ± 0.08	24
N	−83.6 ± 0.9	3.2 ± 0.1	8
K	−94.2 ± 3.6	2.6 ± 0.5	5
H	−76.0 ± 6.3	3.1 ± 0.2	5
R	−72.8 ± 2.8	3.0 ± 0.2	4
E	−96.1 ± 3.2	3.1 ± 0.23	4
D	−98.5 ± 2.3	3.3 ± 0.4	10

Tail current voltage-activation relations were obtained for most mutants using 50 mM Rb^+ as the external charge carrier and fit with single Boltzmann functions. P475D was obtained using 50 mM K^+ as the external charge carrier. P475L results in undetectable ionic or gating currents and P475A results in gating currents but no ionic currents (i.e., a nonconducting mutant). *n* corresponds to the number of experiments.

negative voltages (fractional constitutive conductance $<10^{-4}$) even though they display greatly altered conductance (G)-voltage (V) relations (Fig. 3 C, Table I).

It is evident from Fig. 3 that most of the mutations perturb the closed-open equilibrium in favor of the closed state (i.e., rightward shift of the G-V relation) and exhibit no constitutive conductance, or favor the open state and produce a detectable constitutive conductance. To further examine the relationship between substitutions at P475 and the gating properties of the channel we calculated the free energy difference between closed and open states at 0 mV (ΔG_0) from both the midpoint (V_{50}) and slope (z) of the G-V relation (Table I; Fig. 4). The ΔG_0 quantity does not account for the constitutive conductance because it relies only on the voltage dependence of the channel. Fig. 4 shows plots of either side-chain volume or solvation energy, a measure of the energetics of side-chain transfer from cyclohexane to water (Fersht, 1999), against $\Delta\Delta G_0$ ($\Delta G_0^{mut} - \Delta G_0^{wt}$), with the constitutively conducting mutants demarcated using red symbols. There are several revealing trends evident in these plots. First, larger side chains tend to favor the open state, as indicated by more negative values of $\Delta\Delta G_0$. This trend is particularly evident among residues that do not give rise to a constitutive conductance (e.g., Ser, Cys, Val, Ile, Met, Phe,

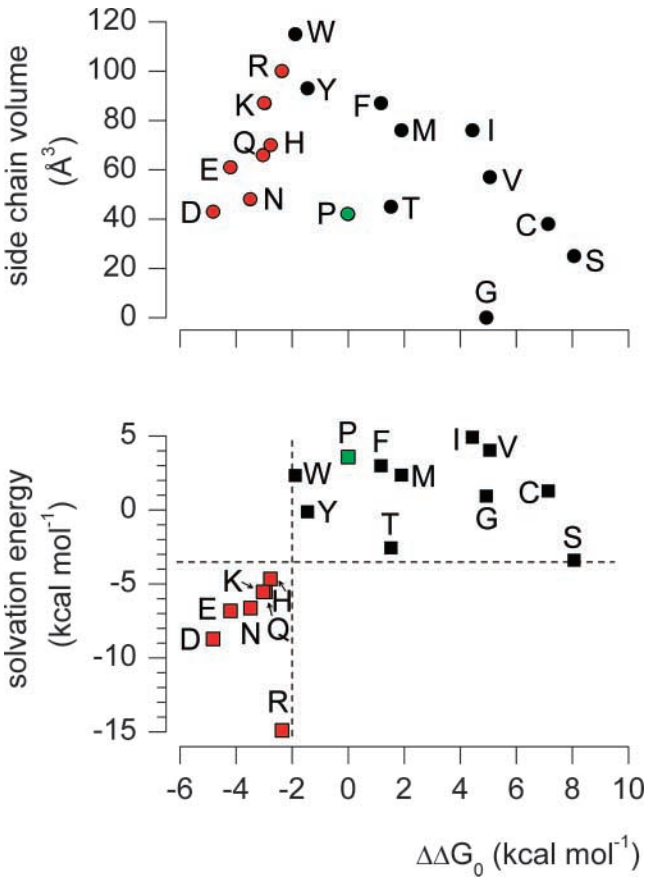

FIGURE 4. Side chain dependence of gating phenotype for substitutions at P475 in the Shaker Kv channel. Plots of either side chain volume or solvation energy against $\Delta\Delta G_0$. Solvation energy is a measure of the energetics of side chain transfer from cyclohexane to water (Fersht, 1999). Both plots have the same x-axis. Mutants that exhibit constitutive conduction are indicated with red symbols and the wild-type Pro residue is indicated with a green symbol. $\Delta\Delta G_0 = (\Delta G_0^{mut} - \Delta G_0^{wt})$ where $\Delta G_0 = zFV_{50}$, with z and V_{50} values from Table I and F is Faraday's constant. P475L results in undetectable ionic or gating currents and P475A results in gating currents but no ionic currents (i.e., a nonconducting mutant). In the bottom plot, dashed black lines are drawn at $\Delta\Delta G_0 = -2$ kcal mol^{-1} and solvation energy $= -3.5$ kcal mol^{-1} to illustrate the clustering of mutations into two regions of the plot.

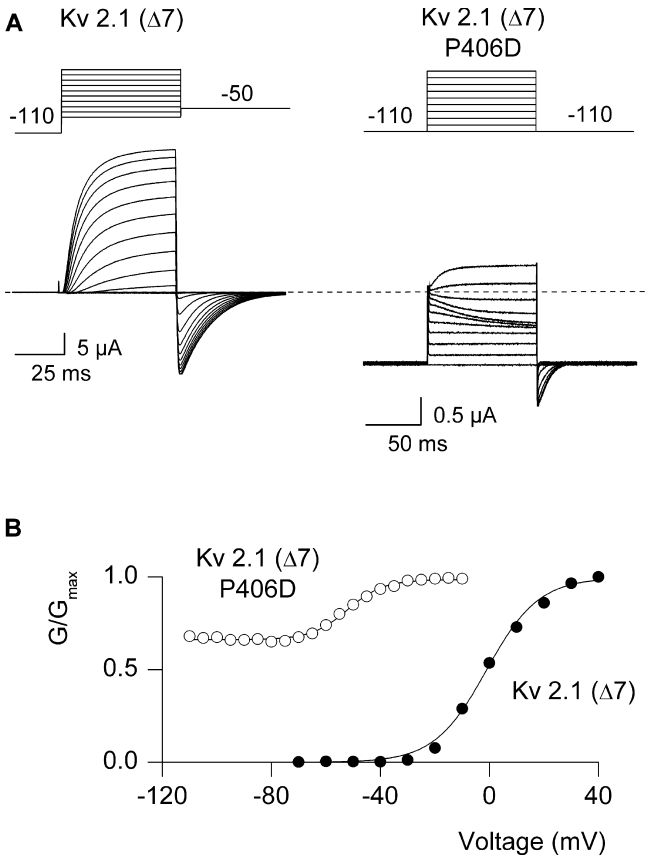

FIGURE 5. Constitutive-conducting phenotype for the P406D mutant in the Kv2.1 channel. (A) Family of ionic currents for Kv2.1 Δ7 and P406D Kv2.1 Δ7. Depolarizations were from −70 to +20 mV (10-mV increments) for Kv2.1 Δ7 and from −110 to −10 mV (10-mV increments) for P406D Kv2.1 Δ7. Charge carrier in the external solution was 50 mM Rb^+. Linear capacity and background conductances were identified and subtracted by blocking the Kv2.1Δ7 channel with Agitoxin-2. Horizontal dashed lines correspond to the zero current level. (B) G-V relations obtained by plotting normalized tail current amplitudes against test voltage. Same cells as in A. Smooth curves are single Boltzmann fits to the data with parameters as follows: Kv2.1 Δ7, $V_{50} = -1.1$ mV, $z = 2.7$; P406D Kv2.1 Δ7, $V_{50} = -52$ mV, $z = 2.7$.

Tyr, Trp). Second, residues with the most negative $\Delta\Delta G_0$ values also have the most negative solvation energies (i.e., high hydrophilicity), and vice versa. This relationship is such that residues cluster together into two defined regions of the $\Delta\Delta G_0$ vs. solvation energy plot. If $\Delta\Delta G_0 < -2$ kcal mol^{-1}, the solvation energy is less than -3.5 kcal mol^{-1}, and the channel exhibits a constitutive conductance. In contrast, if $\Delta\Delta G_0 > -2$ kcal mol^{-1}, the solvation energy is greater than -3.5 kcal mol^{-1}, and the channel exhibits an undetectable level of constitutive conductance. We will return to these interesting patterns in the discussion after presenting experiments addressing the mechanism of constitutive conduction.

Effects of Hanatoxin on a Constitutively Conducting Mutant in the Kv2.1 Channel

The voltage independence of the macroscopic conductance that we observe at negative voltages for the constitutively conducting mutants suggests that ion conduction can occur irrespective of the conformation of the voltage sensor. Hanatoxin is a spider toxin that binds to the four voltage-sensing domains in the Kv 2.1 channel and shifts activation to more depolarized voltages (Swartz and MacKinnon, 1997a; Li-Smerin and Swartz, 2000, 2001). If the constitutive conductance is

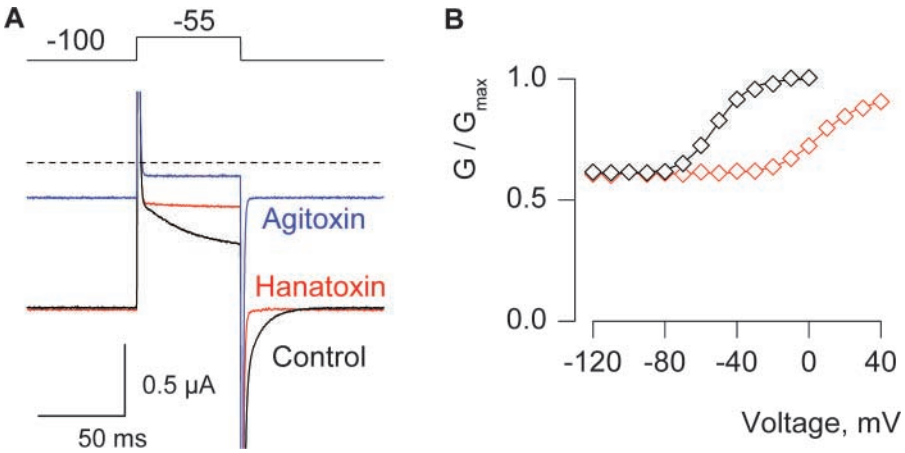

FIGURE 6. Effects of Hanatoxin on the P406D Kv2.1 channel. (A) Current records elicited by weak depolarization in control, Hanatoxin (4 μM) or Agitoxin-2 (100 nM). Traces are shown without subtraction of leak or capacitive currents. Charge carrier in the external solution was 50 mM Rb^+. (B) G-V relations for P406D Kv2.1 Δ7 channels in the absence and presence of 4 μM Hanatoxin. Same cell as in A. Currents remaining in the presence of Agitoxin-2 have been subtracted. Smooth curves are single Boltzmann fits to the data with parameters as follows: control, V_{50} = −51.8 mV, z = 2.8; toxin, V_{50} = +5.7 mV, z = 2.3.

independent of the voltage sensors, Hanatoxin would be expected to inhibit the voltage-activated conductance but spare the standing conductance at negative voltages. Because Hanatoxin interacts with the Shaker Kv channel very weakly, we first asked whether mutation of the equivalent Pro in Kv2.1 (P406) gives rise to a constitutively conducting phenotype that is similar to what is observed in the Shaker Kv channel. These experiments were done using the Kv2.1 Δ7 construct (Aggarwal, 1996; Li-Smerin and Swartz, 1998) because the high-affinity binding site for Agitoxin-2 in the outer vestibule of this channel allows us to use this pore-blocking toxin to identify currents associated with the expressed channel, as in the previous experiments with Shaker. As shown in Fig. 5, mutation of P406 in Kv2.1 to Asp results in a channel that displays a constitutive conductance at negative voltages with a fractional constitutive conductance of ∼0.6 in an external solution containing 50 mM Rb^+. Next, we tested the effects of Hanatoxin at a concentration that is nearly saturating for the Kv2.1 channel. As shown in Fig. 6, Hanatoxin binds to the P406D Kv2.1 channel and inhibits the voltage-activated current by shifting activation to more depolarized voltages, similar to what is observed for the wild-type Kv2.1 channel (Swartz and MacKinnon, 1997a; Li-Smerin and Swartz, 2000, 2001). However, even though Hanatoxin shifts activation by more than 50 mV, the toxin has no effect on the constitutive conductance. These results confirm that the constitutive conductance is independent of the voltage sensors.

Testing for Movement of the Intracellular Pore with the NH_2-terminal Inactivation Domain

One of the potential mechanisms underlying constitutive conduction that would be consistent with the results presented thus far is that the structure of the S6 activation gate has been completely disrupted so that it no longer participates in gating. In this case, the gating that remains (e.g., Figs. 2 and 3) might reflect the action of a gate elsewhere in the protein. The NH_2-terminal inactivation domain in Shaker is a useful probe for structural changes at the intracellular entrance to the pore because it binds in this region, but only after the activation gate opens (Hoshi et al., 1990; Zagotta and Aldrich, 1990; Zagotta et al., 1990; Demo and Yellen, 1991; MacKinnon et al., 1993; Murrell-Lagnado and Aldrich, 1993a,b; Zhou et al., 2001a). If the S6 inactivation gate has been disrupted, the inactivation ball might block the channel with only weak voltage dependence, or possibly it might not block it at all, depending on how drastically the structure in this region has been altered. We therefore asked whether the P475Q mutant of Shaker, a channel that displays both robust constitutive and voltage-dependent activity in extracellular solutions containing 50 mM Rb^+ (Fig. 7 A), undergoes fast inactivation if the NH_2-terminal inactivation domain is intact. Fig. 7 B shows that when the inactivation ball is present in the NH_2 terminus the voltage-activated macroscopic conductance inactivates. The kinetics of inactivation are somewhat slower (∼3-fold) for the P475Q mutation compared with the wild-type channel when examined at positive voltages where inactivation exhibits no apparent voltage dependence (Fig. 7, B and D). This result is not surprising if we consider that the inactivation ball is thought to bind in the vicinity of this residue (Zhou et al., 2001a). The apparent voltage dependence of inactivation during test depolarizations closely follows the voltage-activation relation (Fig. 7 E), consistent with the open state dependence to inactivation, and therefore indicating that the activation gate moves during the test depolarization.

In addition to promoting inactivation of the voltage-activated conductance, membrane depolarization also results in a reduction of the constitutive current at −150 mV. This observation is most clearly seen after re-

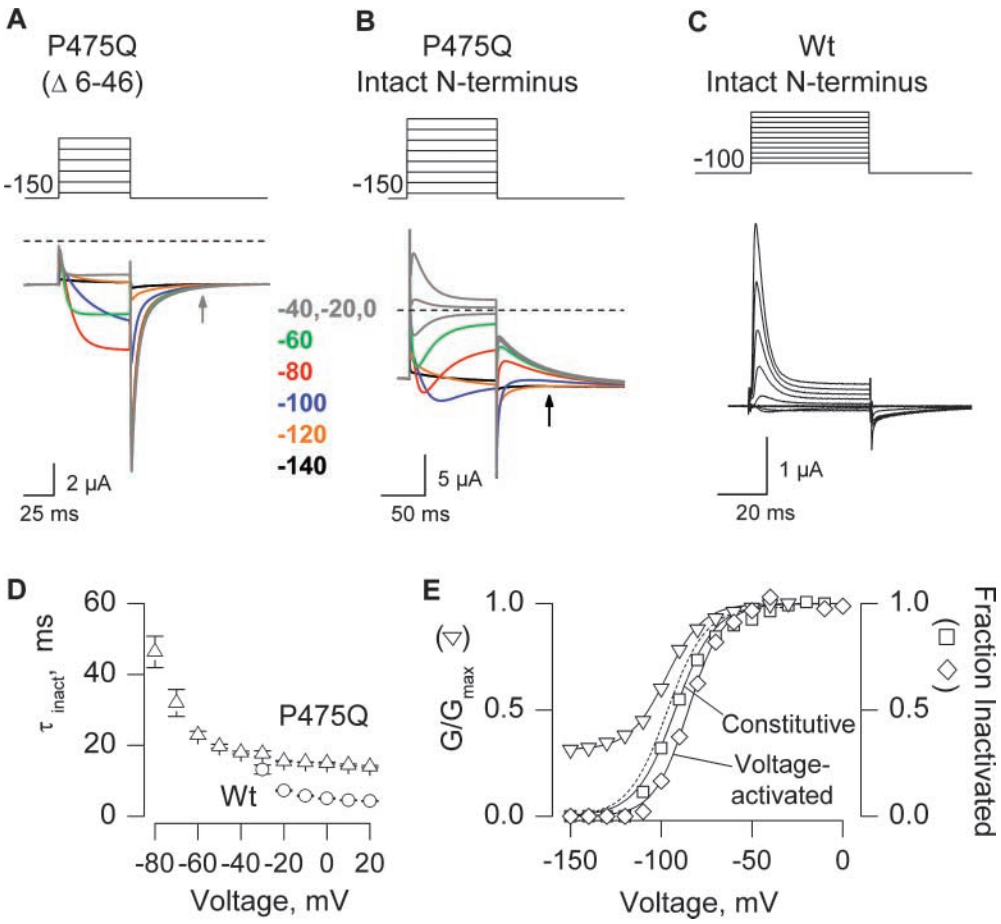

FIGURE 7. N-type inactivation in the P475Q Shaker Kv channel. (A) Family of ionic currents for P475Q with deletion of residues 6–46. The cell was held at −100 mV, stepped to −150 mV for 200 ms before the traces shown, tail voltage was −150 mV, and depolarizations were between −140 and −40 mV in 20-mV steps. Linear capacity and background conductances were identified and subtracted by blocking the Shaker channel with Agitoxin-2. Horizontal dashed lines correspond to the zero current level. Charge carrier in the external solution was 50 mM Rb^+. (B) Family of ionic currents for P475Q with an intact NH_2-terminal inactivation ball. Same protocol and conditions as in A except that depolarizations were to between −140 and 0 mV in 20-mV steps. (C) Family of ionic currents for the wild-type Shaker channel with an intact NH_2-terminal inactivation domain. Same conditions as in A except that depolarizations were from −80 to +20 mV (10-mV steps). (D) Kinetics of inactivation for wild-type and P475Q channels. Inactivation during the test pulses in B and C was fit with single exponential functions and the resulting time constants (τ) plotted against test voltage. $n = 5$ for both wild-type and P475Q. (E) Voltage dependence for activation and N-type inactivation. Open triangles, normalized tail current amplitude (measured in A) plotted against test voltage. Smooth black curve is a single Boltzmann fit to the G-V data with $V_{50} = -97$ mV, $z = 2.5$ with a fractional constitutive conductance of 0.31. Dashed black curve is a simulated G-V normalized to remove the constitutive conductance. Open squares, normalized fractional inactivation of the constitutive current at −150 mV plotted against voltage of the preceding test depolarization. Inactivation of constitutive current was measured at the black arrow in B, at which time deactivation in Δ6–46 (gray arrow in A) is nearly complete. Smooth curve is a single Boltzmann fit to the inactivation data with $V_{50} = -92$ mV, $z = 2.3$. Open diamonds, normalized fractional inactivation during the test depolarization (measured as the difference between the peak and steady-state currents in B) plotted against voltage of the test depolarization. Smooth black curve is a single Boltzmann fit to the inactivation data with $V_{50} = -85$ mV, $z = 2.7$.

polarization where recovery from inactivation is evident (Fig. 7 B). If we measure the fractional inactivation of the constitutive current 60 ms after repolarization to −150 mV (Fig. 7 B, black arrow), a time point at which the control channel has nearly completely deactivated (Fig. 7 A, gray arrow), and plot against the voltage of the test depolarization, the observed voltage dependence closely follows the voltage-activation relation (Fig. 7 E). The steep voltage dependence observed here implies (a) that the conducing state of the channel that exists at negative voltages is relatively insensitive to the inactivation domain; and (b) that the conducting state at negative voltages is in rapid equilibrium with the conducting state observed at depolarized voltages, after voltage-sensor activation. The observed inactivation of both the voltage-dependent and constitutive conductances strongly suggests that the structure of the intracellular entrance to the pore changes conformation during the process of activation.

Single Channel Properties of Two Constitutively Conducting Mutants

The results presented thus far suggest that the constitutive conduction is independent of the voltage-sensors, yet the S6 gate still changes conformation with membrane depolarization. Another potential mechanism that would be consistent with these findings is that the intracellular activation gate undergoes its normal conformational change but can no longer effectively mini-

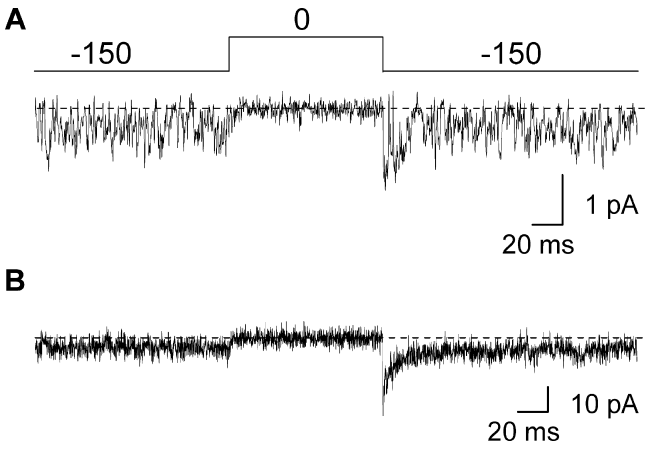

FIGURE 8. Single-channel properties of the Shaker P475Q mutant channel recorded in symmetrical Rb^+. (A) Single-channel currents recorded for P475Q in symmetrical 140 mM RbCl. The single-channel patch shown was held at −100 mV and stepped to −150 mV for 350 ms before the traces shown. Filter frequency was 2 kHz. Horizontal dashed lines correspond to the zero current level. (B) Ensemble of 15 single channel sweeps from the same patch shown in A and elicited using the same protocol as in A.

mize the flow of ion when in the "closed" conformation. Previous estimates suggest that the conductance of the closed state of the Shaker Kv channel is at least 10^5 lower than for the open state of the channel (Soler-Llavina et al., 2003). Perhaps these mutations increase the conductance of the closed state to readily measurable values. To evaluate this possibility we studied the unitary properties of both Shaker P475Q and P475D, two mutant channels with different degrees of constitutive activity at negative voltages (Figs. 2 and 3). As will become evident, the constitutively conducting mutants exhibit rather complex single channel behavior, with rapid transitions between different apparent conductance levels that are poorly resolved. We use the term "apparent" because these lower conductance levels might correspond to brief openings whose measured amplitude has been decreased by filtering. Our goal here is not to explore the channel kinetics in detail, but to examine whether the channel can close completely.

We initially examined the unitary properties of P475Q in symmetrical 140 mM Rb^+ and observed channel activity that displayed very rapid transitions between different apparent conductance levels (Fig. 8 A). This type of activity was not observed in patches pulled from uninjected oocytes or when Agitoxin-2 was included in the patch pipette ($n = 17$). Thus, we are confident that the observed activity arises from the Shaker Kv channel. Although ensemble averaging of the activity observed for Shaker P475Q yields a fractional constitutive conductance (Fig. 8 B) that agrees with macroscopic recordings (Fig. 3), it is difficult to ascertain whether the mutant can close completely.

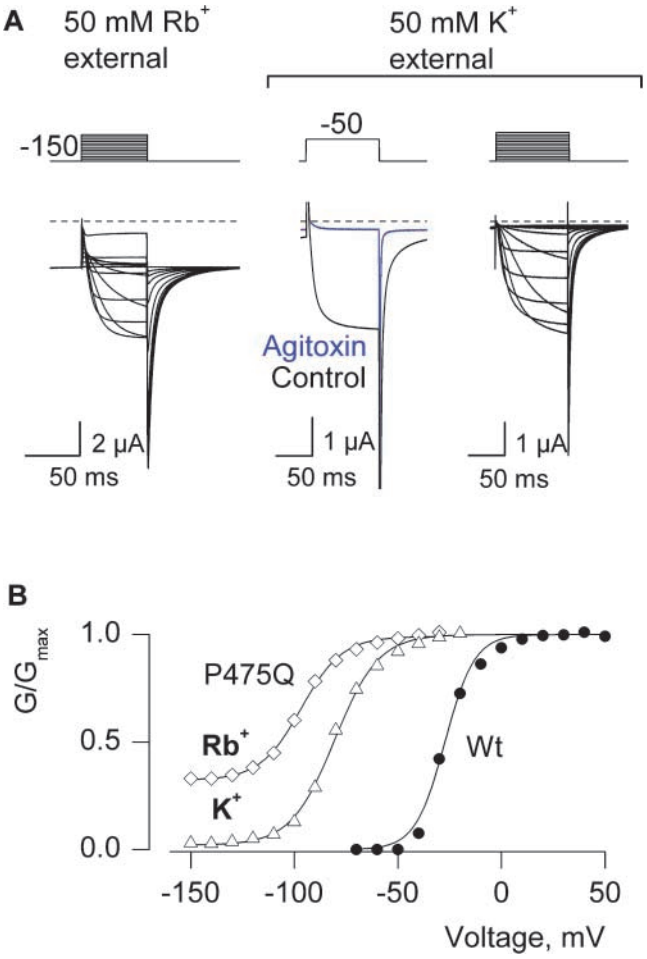

FIGURE 9. Permeant ion dependence of constitutive conduction for P475Q. (A) Families of ionic currents for Shaker P475Q with either 50 mM Rb^+ or 50 mM K^+ as the external permeant ion. The recordings for external Rb^+ and K^+ are from different cells. In each case the membrane was held at −100 mV and stepped to −150 mV for 200 ms before the traces shown and tail voltage was −150 mV. Depolarizations were from −150 to −20 mV in 10-mV steps for both left and right families. For these families both linear capacity and background conductances were identified and subtracted by blocking the Shaker channel with Agitoxin-2. Horizontal dashed lines correspond to the zero current level. Middle two traces are uncorrected currents elicited by depolarization to −50 mV in either control or Agitoxin-2 with K^+ as the external permeant ion. (B) G-V relations obtained by plotting normalized tail current amplitudes against test voltage for Wt and P475Q in external Rb^+ and K^+. Smooth curves are single Boltzmann fits to the data with parameters as follows: Wt (Rb^+ external), $V_{50} = -27.3$ mV, $z = 3.6$; P475Q (Rb^+ external), $V_{50} = -96.7$ mV, $z = 2.6$; P475Q (K^+ external), $V_{50} = -80.5$ mV, $z = 2.4$.

In two electrode voltage clamp recordings we observed that the fractional constitutive conductance is not fixed for a given mutant, but varies considerably with the species of permeant ion in the extracellular solution (Fig. 9). In the case of P475Q, the fractional constitutive conductance is 0.3 when 50 mM Rb^+ is the external charge carrier, but only 0.05 in 50 mM

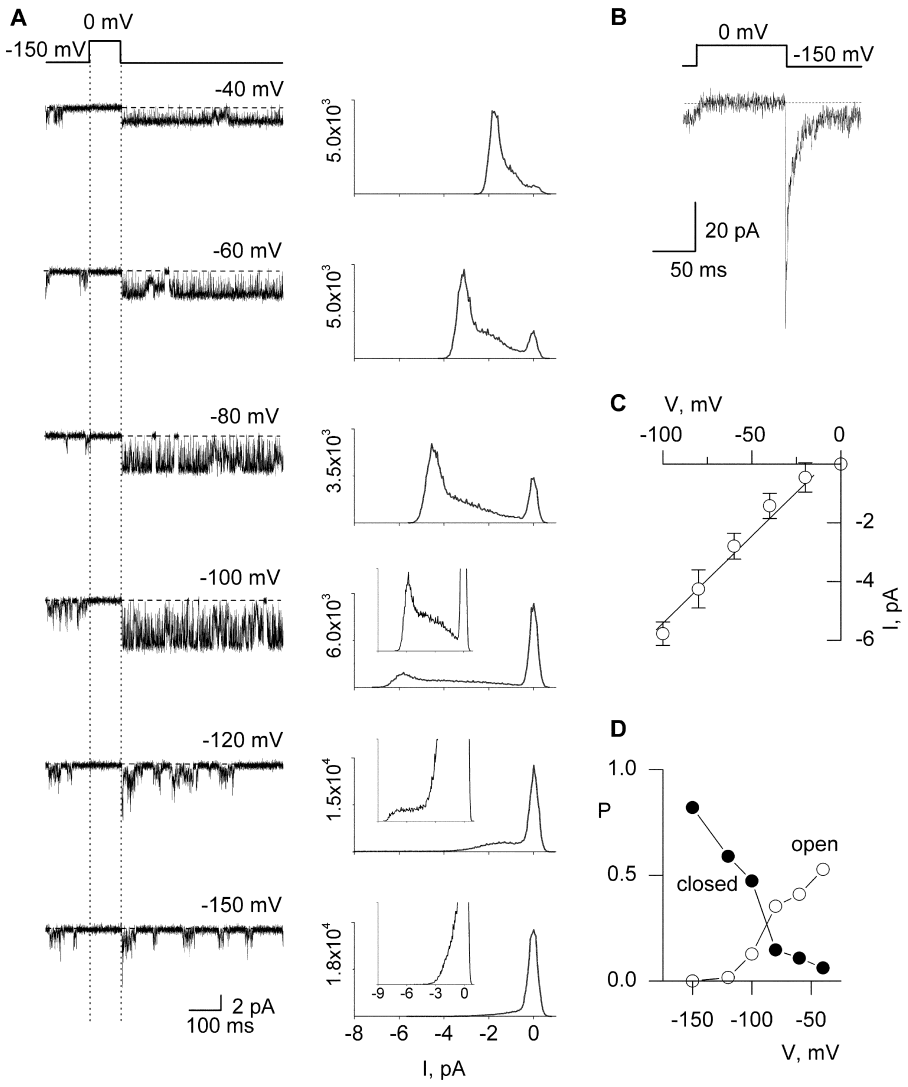

FIGURE 10. Single-channel properties of the Shaker P475Q mutant channel recorded in symmetrical K^+. (A) Representative current traces (left) and corresponding all points amplitude histograms (right) recorded in symmetrical 140 mM KCl. The single channel patch shown was held at −100 mV and stepped to −150 mV for 350 ms before the traces shown. Filter frequency was 2 kHz. Horizontal dashed lines correspond to the zero current level. Y-axes for histograms are number of events and each histogram contains data from 6–10 sweeps. For inset histograms, y-axes range from 0 to (from top to bottom) 10^3, 5×10^2, and 10^3. (B) Ensemble of 30 single-channel sweeps from the same patch shown in A and elicited using the same protocol as in A. (C) i-V relationship for the highest conducting state. Each data point represents the mean ± SD ($n = 6$). Linear regression of the data shown yields a conductance of 60 pS. (D) Probability (P) for the closed and highest conducting open state as a function of voltage. All point histograms in A were fit with multiple Gaussians and their relative areas used to estimate probabilities.

external K^+ (Fig. 9). In addition to a difference in the extent of constitutive conductance, the midpoint of the G-V relation in Rb^+ is shifted to more negative voltages by ~13 mV when compared with recordings in external K^+ (Fig. 9 B). Although the standing conductance at negative voltages is small in the presence of external K^+, its sensitivity to Agitoxin-2 (Fig. 9 A) distinguishes it from leak or endogenous conductances. To look for evidence of complete closure we examined the unitary properties of P475Q using K^+ as the external permeant ion. The much smaller fractional constitutive conductance observed with external K^+ might be expected to make closures more frequent, and thus easier to discern. Channel activity similar to that illustrated in Fig. 10 was observed for P475Q in eight single-channel patches in the presence of 140 mM symmetrical K^+. The highest conductance level for P475Q was estimated to be 60 pS (Fig. 10, A and C), compared with ~24 pS for the wild-type channel under similar ionic conditions (Heginbotham and MacKinnon, 1993). P475Q could be seen to enter quiescent states where no apparent activity was observed for several minutes (unpublished data), presumably because the channel entered a slow-inactivated state. When active, the mutant channel opens to multiple apparent conductance levels (Fig. 10 A). At −150 mV the channel opens to apparent subconductance levels that can be seen as a broad tail in the all points histograms (Fig. 10 A) and exhibit a probability of ~0.18. Importantly, under these ionic conditions there are events in the unitary recordings where the channel appears to close completely. These events are relatively frequent, with a probability of being closed around 0.8 at −150 mV (Fig. 10, A and D). No such activity was observed in uninjected oocytes. The P475Q mutant also exhibits further activation with depolarization of the membrane (Fig. 10 A), with the probability of residing in the highest conducting level showing clear voltage dependence (Fig. 10 D). If the apparent closed events that we observed for P475Q

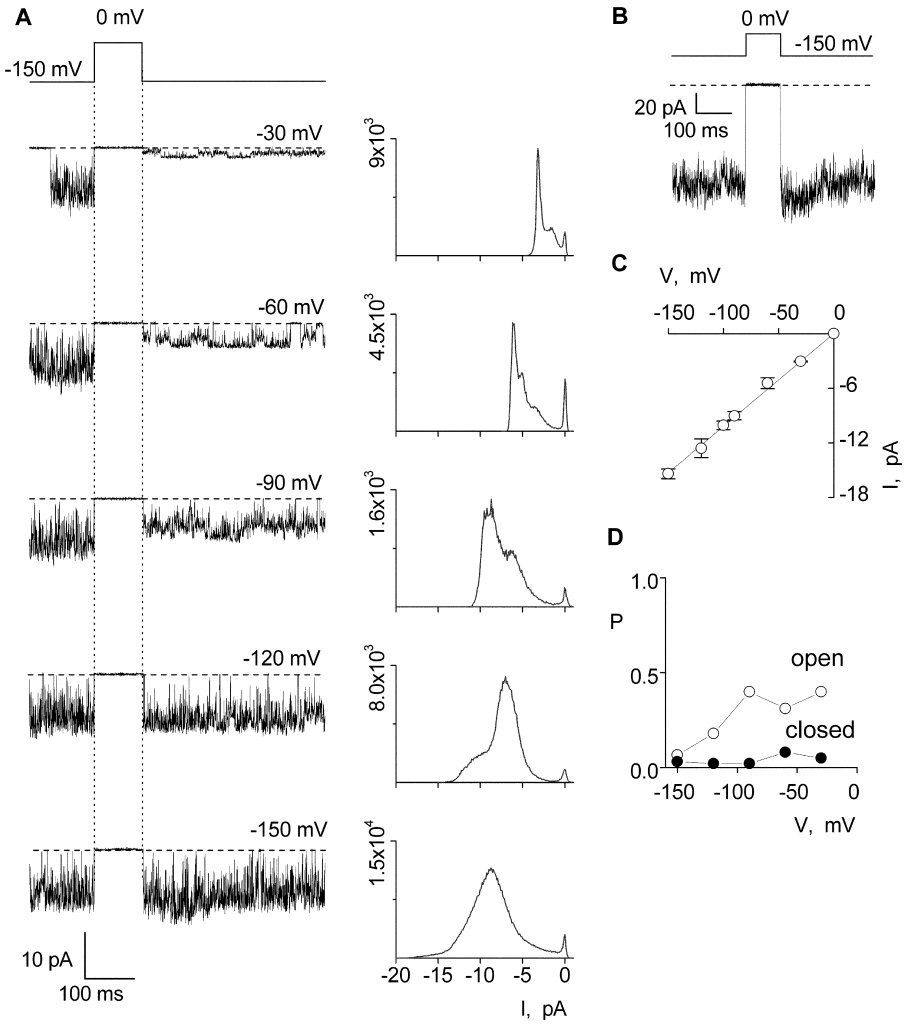

FIGURE 11. Single-channel properties of the Shaker P475D mutant channel recorded in symmetrical K^+. (A) Representative current traces (left) and corresponding all points amplitude histograms (right) recorded in 140 mM symmetrical KCl. The single channel patch shown was held at −100 mV and stepped to −150 mV for 350 ms before the traces shown. Filter frequency was 1 kHz. Horizontal dashed lines correspond to the zero current level. Y-axes for histograms are number of events and each histogram contains data from 6–10 sweeps. (B) Ensemble of 11 single-channel sweeps elicited using the same protocol as in A. (C) i-V relationship for highest conducting open state. Each data point represents the mean ± SD (n = 4). Linear regression of the data shown yields a conductance of 100 pS. (D) Probability (P) for the closed and highest conducting open state as a function of voltage. All point histograms in A were fit with multiple Gaussians and their relative areas used to estimate probabilities.

correspond to states of the channel that are effectively nonconducting, they could not contribute to the constitutive conductance seen in macroscopic recordings. In this case, the observed openings should be able to account for the fractional constitutive conductance in macroscopic recordings. The openings at −150 mV occur with a probability of 0.18 and have a unitary conductance of ~15 pS, whereas the openings at more positive voltages have a probability of 0.9 and are dominated by openings to the main conductance level (60 pS). The fractional constitutive macroscopic conductance predicted from these values is 0.05, a value that is comparable to the fractional constitutive conductances measured from macroscopic recordings with K^+ as the charge carrier (0.05; Fig. 9, A and B) and from tail currents in single-channel ensembles (0.06; Fig. 10 B).

If the gate in the constitutively conducting mutants is capable of full closure, we would predict that the observed closed events for P475D would be more infrequent compared with P475Q because the P475D mutant has a much larger fractional constitutive conductance in macroscopic current recordings (~0.9; Fig. 2). We therefore examined the unitary properties of the P475D mutant in symmetrical K^+ (140 mM) and observed channel activity similar to that illustrated in Fig. 11 in four single-channel patches. The highest apparent conductance level is ~100 pS for P475D (Fig. 11, A and C) and the channel entered quiescent states where no apparent activity was observed, similar to P475Q. For P475D, the fractional constitutive conductance from single-channel ensembles and macroscopic recordings are both ~0.9 (Figs. 2 B and 11 B). As predicted, in the case of P475D there are infrequent events (probability ~0.03) where the channel appears to close completely. We conclude that the apparent closures observed in unitary recordings correspond to states when the Shaker channel is for all intensive purposes nonconducting. These findings would seem to rule out the possibility that constitutive conduction arises from a leaky gate. In the discussion we will explore how the present results can be understood if the mutations have pronounced effects on the closed to open equilibrium.

The objective of this study was to explore the mechanism by which mutations within the S6 activation gate give rise to a constitutive macroscopic conductance in Kv channels. In Shaker, this phenotype is not observed for all substitutions at P475, but occurs only after substitution of the most hydrophilic amino acids, including Asp, Glu, Gln, Asn, His, Lys, and Arg (Figs. 3 and 4). We observed a very similar phenotype in the related Kv2.1 channel when we mutated the equivalent Pro to Asp (Fig. 5). In this Kv channel our experiments with Hanatoxin, a gating modifier that interacts with the voltage-sensing domains of the channel, suggest that this constitutive conductance is independent of the voltage-sensors (Fig. 6).

Constitutive Conduction by Disruption of the S6 Gate

One of the mechanisms that we examined was that hydrophilic substitutions at P475 completely disrupt the intracellular S6 activation gate. If the S6 gate were destroyed in the constitutively conducting mutants then another gate, perhaps the selectivity filter (Chapman et al., 1997; Zheng and Sigworth, 1997, 1998; Zhou et al., 2001b), would need to be invoked to explain the variable extent of voltage-dependent gating that remains. In the case of P475N with Rb^+ as the external permeant ion (Fig. 3) and P475Q with K^+ as the external permeant ion (Fig. 9), the fractional constitutive conductances are sufficiently small that they would be impossible to define were it not for our use of the Agitoxin subtraction procedure. It seems unlikely that the large extent of gating that remains in these mutants could be explained by gating of the selectivity filter since only relatively small changes in single channel conductance have been attributed to gating at the selectivity filter (Chapman et al., 1997; Zheng and Sigworth, 1997, 1998; Zhou et al., 2001b). A nonconductive conformation of the selectivity filter has been observed in X-ray structures of the KcsA K^+ channel solved in low concentrations of K^+ (Zhou et al., 2001b). In this instance, gating at the selectivity filter was proposed to occur via the ability of the intracellular S6 gate to regulate the access of K^+ to the filter. This scenario would predict that full disruption of the S6 gate would uncouple gating at the selectivity filter and result in unregulated constitutive conduction, counter to what we observe for most mutants at P475. Although complete abolition of one of two gates probably cannot explain our results for all substitutions at P475, it is possible that for the most extreme mutants (i.e., P475D and E), where the macroscopic conductance changes relatively little as a function of membrane voltage, the intracellular gate plays little or no role in the gating of ions.

Our experiments with the NH_2-terminal inactivation domain in the Shaker Kv channel show that the P475Q mutant is capable of inactivating. Both the voltage-activated and constitutive conductances exhibit enhanced inactivation with membrane depolarization (Fig. 7). The observed voltage dependence to inactivation in both cases has a similar steepness and position on the voltage axis when compared with voltage-dependent activation (Fig. 7), suggesting that the voltage dependence to inactivation largely arises from coupling between inactivation and activation. (Destabilization of the inactivated state due to K^+ permeation from the external side of the membrane [Demo and Yellen, 1991; Murrell-Lagnado and Aldrich, 1993a; Gomez-Lagunas and Armstrong, 1994] and a small amount of intrinsic voltage dependence to inactivation, could also contribute to the observed voltage dependence.) The lower conducting states observed at negative voltages in single-channel recordings (Figs. 8 and 10) appear to be relatively insensitive to the inactivation domain (Fig. 7), either because they are too short lived or because the structures of these states are distinct from those that exist at depolarized voltages. In either case, the apparent voltage dependence to inactivation in P475Q implies that the S6 gate undergoes a conformational change with membrane depolarization. We conclude that the S6 activation gate has not been completely disrupted by the constitutively conducting mutations.

Constitutive Conduction from a Closed Gate that Conducts

Another mechanism that we tested was whether the conductance of the closed state has been increased by the hydrophilic substitutions. Our analysis of the unitary properties of both P475Q and P475D (Fig. 8–11), two mutants of the Shaker channel with rather different fractional constitutive conductances, suggest that these mutants can enter states that are effectively nonconducting (see results for rationale). In particular, the changes in the probability and conductance of the observed openings can readily account for the fractional constitutive conductances measured from macroscopic conductances, arguing against undetected conduction during the apparent closures. When taken together with conformational changes in the intracellular pore detected with the inactivation domain, these results suggest that the intracellular gate closes and is capable of decreasing the flow of ions to levels that are insignificant for the purposes of the present discussion.

Constitutive Conduction by Perturbation of the Closed-open Equilibrium

The mechanism that is the most compatible with our results is that mutations at P475 produce a dramatic perturbation of the closed to open equilibrium. We will discuss this possibility in the context of two relatively

simple gating schemes that are conceptually useful in thinking about the mechanism of constitutive activation. There is considerable evidence for a general model of Kv channel activation, illustrated in Scheme I, in which each of the four subunits undergoes a voltage-dependent conformational change independently, followed by a weakly voltage-dependent concerted transition (Hoshi et al., 1994; Zagotta et al., 1994a,b; Schoppa and Sigworth, 1998a,b,c; Smith-Maxwell et al., 1998a,b; Ledwell and Aldrich, 1999; Horn et al., 2000; Mannuzzu and Isacoff, 2000).

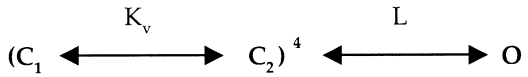

SCHEME I

The independent transition between C_1 and C_2 is governed by the equilibrium constant K_v and is presumed to correspond to movements of the four voltage sensors, whereas the concerted transition is governed by L and is presumed to reflect opening of the S6 activation gate. A dramatic perturbation of the final opening transition in Scheme I would predict a shift of the voltage-activation relation to more negative voltages, as we observed (Figs. 2–5, and 9), but cannot account for constitutive openings because the transition governed by K_v would drive the open probability to very low values once a sufficiently negative voltage is applied. In addition, the insensitivity of the constitutive conductance to Hanatoxin, a toxin that is thought to influence the transition between C_1 and C_2 (Swartz, 2001), cannot be explained in Scheme I because stabilization of C_1 by the toxin would inhibit the constitutive conductance. A modified allosteric model for activation of Kv channels is depicted in Scheme II whereby the channel can open either before or after voltage-sensor activation (see Lu et al., 2002, for additional discussion). In this scheme, voltage-dependent gating can be produced simply by making L much larger than L′. One way to explain our results in the context of this scheme would be that hydrophilic substitutions at P475 perturb the closed to open equilibrium in such a way that the equilibrium constants L and L′ change dramatically. If we assume that L and L′ are voltage independent, then Scheme II could account for opening of the channel before voltage-sensor activation and a leftward shift in the G-V relation. The variation in the fractional constitutive conductance with different substitutions (e.g., Gln vs. Glu) could be explained by the extent to which mutations perturb both L and L′. The Hanatoxin insensitivity of the constitutive conductance can be explained by Scheme II if the toxin affects Kv and Kv′ equally. The effects of external permeant ions on the fractional constitutive conductance (Fig. 9) might be related to the "foot in the door" effect studied by Armstrong and coworkers, where they proposed that the intracellular activation gate cannot close with an ion in the aqueous cavity (Swenson and Armstrong, 1981; Matteson and Swenson, 1986; Doyle et al., 1998; Melishchuk and Armstrong, 2001). If the dwell time of Rb^+ in the cavity is greater than K^+, then one would predict differential effects of these permeant ions on the closed-open transitions in Scheme II. Our unitary recordings of P475Q with external Rb^+ and K^+ show a higher constitutive open probability with Rb^+ (Figs. 8 and 10), a finding that is to a first approximation consistent with both the "foot in the door" model and Scheme II.

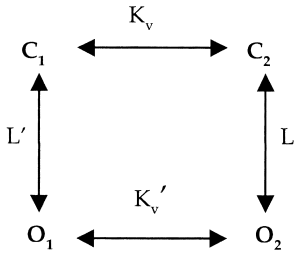

SCHEME II

In the simplest form of Scheme II, the structure of the intracellular activation gate is equivalent for the two open states (O_1 and O_2). However, there are two observations that point to a possible structural difference between the open states that occur before and after voltage-sensor activation. First, our results in Fig. 7 suggest that the open state before voltage-sensor activation (O_1) is relatively insensitive to inactivation (see previous discussion). Second, the openings that occur before voltage-sensor activation correspond to what appear to be subconductance levels. Although both the inactivation and the subconductance findings can also be explained by brief open events, we cannot exclude the possibility of two structurally distinct open states.

There is another way to understand the present observations using a concept of coupling between conformational changes in the voltage sensors and the activation gate. In Scheme II, these two types of conformational changes are coupled by virtue of the fact that the equilibrium constants for conformational changes in the gate (L and L′) depend on the conformation of the voltage sensor, and vice versa. In this scheme the strength of coupling can be defined by a coupling constant that is equal to the ratio of L to L′ which thermodynamically must also equal the ratio of K_v to K_v'. What is known about the strength of coupling in the wild-type Shaker Kv channel? Single-channel recordings of Shaker show steeply voltage-dependent open probabilities down to values as low as 10^{-9} at negative membrane voltages (Islas and Sigworth, 1999) and a maximal open probability at positive voltages ~0.8–0.9 (Hoshi et al., 1994; Zagotta et al., 1994b; Schoppa and Sigworth, 1998a; Islas and Sigworth, 1999), pointing to a ratio for L to L′ of $>10^9$. However, macroscopic recordings for

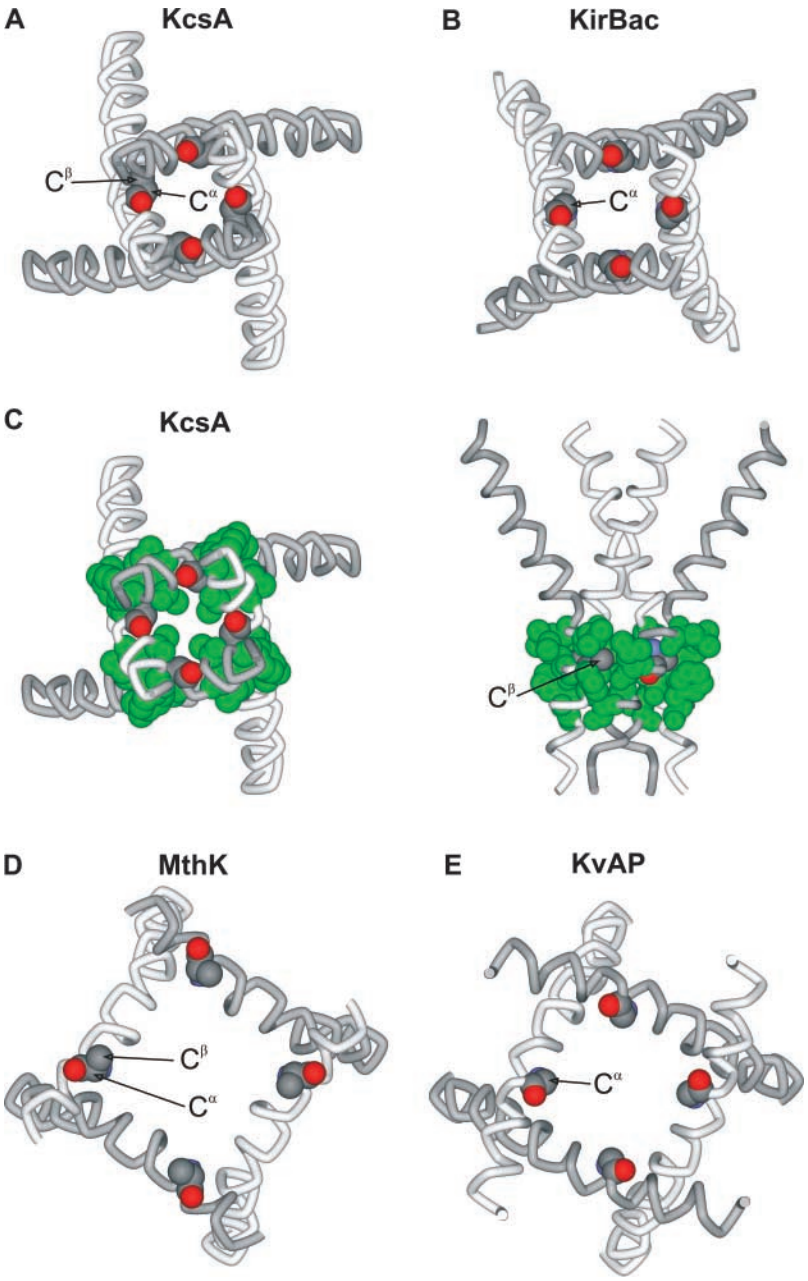

FIGURE 12. Structures of the inner helices in four types of K^+ channels. (A) Inner helices (TM2) of KcsA from an intracellular view with the atoms of A108 represented as CPK. PDB accession code 1J95. (B) Inner helices (TM2) of KirBac from an intracellular view with the atoms of G143 represented as CPK. PDB coordinates generously provided by Declan A. Doyle. (C) Similar representation of KcsA as in A, except surrounding hydrophobic residues (L105, L110, A111, and F114) are represented as CPK and colored green. (D) Inner helices (TM2) of MthK from an intracellular view with the atoms of E92 (modeling as Ala) represented as CPK. PDB accession code 1LNQ. (E) Inner helices (S6) of KvAP from an intracellular view with the atoms of G229 represented as CPK. PDB accession code 1ORQ. Structures were generated using DS Viewer Pro (Accelrys).

cells expressing large numbers of Shaker channels suggest that the minimal open probability at negative voltages could be as high as 10^{-5} if the kinetics of the C_1 to O_1 transitions are sufficiently rapid so as to be unseen in single-channel recordings (Soler-Llavina et al., 2003). Thus, we can estimate that the strength of coupling is $\geq 10^5$. In Scheme II, one could account for most of our observations by an increase in L′ without changing L, an effect that would be tantamount to a change in the strength of coupling. Interestingly, we don't see a significant increase in the maximal open probability for either P475Q or D, perhaps indicating that L remains relatively unaffected. However, it is possible that a second gate such as the selectivity filter serves to limit the maximal open probability, and thus masks a pronounced change in L. We therefore conclude that the constitutively conducting mutants produce a marked change in the closed-open equilibrium, occurring either with or without a change in the strength of coupling. This conclusion is consistent with studies of chimeras between KcsA and Shaker that display a constitutively conducting phenotype (Lu et al., 2001, 2002).

Reflections on K^+ Channel Structure

Can we explain a pronounced effect of hydrophilic substitutions at P475 on the closed to open equilibrium in light of the structures of K^+ channels that have been

solved by X-ray diffraction? From sequence alignments of the inner helices within the activation gate regions of Shaker, KcsA (Doyle et al., 1998), KirBac (Kuo et al., 2003), MthK (Jiang et al., 2002a), and KvAP (Jiang et al., 2003) (Fig. 1 B), we identified residues that appear at positions equivalent to P475 in Shaker and then examined their location and environments in the four known structures (Fig. 12). In the case of both KcsA and KirBac, which both have intracellular gate regions that appear closed (Roux et al., 2000; Zhou et al., 2001a; Jiang et al., 2002a; Kuo et al., 2003), the residue at the position equivalent to P475 is located in a relatively tightly packed region of the helical bundle, with C^{α} and C^{β} atoms oriented such that side chains would project directly toward the adjacent inner helix (Fig. 12, A and B). Interestingly, these residues in KcsA and KirBac are surrounded by residues with strong hydrophobic character (green residues in Fig. 12, C). In contrast, in either MthK or KvAP, where the internal pores appear open (Jiang et al., 2002a,b; Jiang et al., 2003), the residues positioned at the equivalent of P475 project into water-exposed regions of the pore (Fig. 12, D and E). This open accessibility of residues at the internal end of the inner helix is largely due to the fact that the intracellular portions of the inner helices move away from the central pore axis (and thus each other) in the open state. In light of these dramatically different environments between open and closed states, it is not surprising that large hydrophilic substitutions would destabilize the closed state and have little if any effect on the open state. This structural picture is remarkably consistent with the observed relationships between gating phenotype and both side chain volume and solvation energy (Fig. 4), which suggest that P475 is located in a restricted hydrophobic environment in the closed state, but an aqueous and less confined environment in the open state. The pronounced effects on gating that we observed here are probably unrelated to the known effects of Pro residues on the stability of α-helices. Many substitutions at 475 have only very small effects on the closed to open equilibrium even though their known effects on helix stability are very different than Pro (Figs. 3 and 4; Table I).

It has been suggested that the S6 helix in Shaker is kinked by the presence of a Pro-Val-Pro motif that is absent from the four prokaryotic K^+ channels discussed above (Holmgren et al., 1998; del Camino et al., 2000; del Camino and Yellen, 2001). In the closed state of Shaker, the environment around P475 is likely to be hydrophobic even if there is a kink in the S6 helix because the hydrophobic residues discussed above (Fig. 12 C) are well conserved in all K^+ channels, including Shaker (Fig. 1 B). In addition, mutagenesis studies in Shaker's activation gate suggest that the region around P475 is likely to be tightly packed and crowded in the closed state (Hackos et al., 2002; Yifrach and MacKinnon, 2002). If the movements of the activation gate in Shaker are roughly similar to what has been proposed from the structures of MthK and KvAP, the region around P475 will be water exposed and less crowded in the open state. Thus, to a first approximation, the simple structural explanation for the effects of large hydrophilic substitutions will likely be applicable for all K^+ channels.

Conclusion

The results presented here show that hydrophilic substitutions within the activation gate region of the Shaker Kv channel cause a dramatic destabilization of the closed state of the gate. This perturbation is sufficiently profound that the gate can open even though the voltage sensors remain at rest, supporting an allosteric model for activation of Kv channels and the presence of a voltage-independent closed to open transition in the activation pathway. The proposed mechanism for constitutive activation in the Shaker Kv channel can be understood in light of the X-ray structures of other K^+ channels in this region.

We thank Miguel Holmgren, Mark Mayer, and Shai Silberberg for helpful discussions and critique of the manuscript, and J. Nagle and D. Kauffman in the NINDS DNA Sequencing Facility for DNA sequencing.

Olaf S. Andersen served as editor.

Submitted: 24 July 2003
Accepted: 16 September 2003

REFERENCES

Aggarwal, S.K. 1996. Analysis of the voltage sensor in a voltage-activated potassium channel. Dissertation. Harvard University, Cambridge, MA. 90 pp.

Aggarwal, S.K., and R. MacKinnon. 1996. Contribution of the S4 segment to gating charge in the Shaker K^+ channel. *Neuron.* 16: 1169–1177.

Armstrong, C.M. 1969. Inactivation of the potassium conductance and related phenomena caused by quaternary ammonium ion injection in squid axons. *J. Gen. Physiol.* 54:553–575.

Armstrong, C.M. 1971. Interaction of tetraethylammonium ion derivatives with the potassium channels of giant axons. *J. Gen. Physiol.* 58:413–437.

Armstrong, C.M., and B. Hille. 1972. The inner quaternary ammonium ion receptor in potassium channels of the node of Ranvier. *J. Gen. Physiol.* 59:388–400.

Bezanilla, F. 2002. Voltage sensor movements. *J. Gen. Physiol.* 120: 465–473.

Chapman, M.L., H.M. VanDongen, and A.M. VanDongen. 1997. Activation-dependent subconductance levels in the drk1 K channel suggest a subunit basis for ion permeation and gating. *Biophys. J.* 72:708–719.

del Camino, D., M. Holmgren, Y. Liu, and G. Yellen. 2000. Blocker protection in the pore of a voltage-gated K^+ channel and its structural implications. *Nature.* 403:321–325.

del Camino, D., and G. Yellen. 2001. Tight steric closure at the intracellular activation gate of a voltage- gated K^+ channel. *Neuron.*

32:649–656.
Demo, S.D., and G. Yellen. 1991. The inactivation gate of the Shaker K^+ channel behaves like an open- channel blocker. *Neuron.* 7:743–753.
Doyle, D.A., J.M. Cabral, R.A. Pfuetzner, A. Kuo, J.M. Gulbis, S.L. Cohen, B.T. Chait, and R. MacKinnon. 1998. The structure of the potassium channel: molecular basis of K^+ conduction and selectivity. *Science.* 280:69–77.
Fersht, A. 1999. Structure and Mechanism in Protein Science: A Guide to Enzyme Catalysis and Protein Folding. W.H. Freeman and Co., New York, NY. 631 pp.
Frech, G.C., A.M. VanDongen, G. Schuster, A.M. Brown, and R.H. Joho. 1989. A novel potassium channel with delayed rectifier properties isolated from rat brain by expression cloning. *Nature.* 340:642–645.
Gandhi, C.S., and E.Y. Isacoff. 2002. Molecular models of voltage sensing. *J. Gen. Physiol.* 120:455–463.
Garcia, M.L., M. Garcia-Calvo, P. Hidalgo, A. Lee, and R. MacKinnon. 1994. Purification and characterization of three inhibitors of voltage- dependent K^+ channels from *Leiurus quinquestriatus var. hebraeus* venom. *Biochemistry.* 33:6834–6839.
Gomez-Lagunas, F., and C.M. Armstrong. 1994. The relation between ion permeation and recovery from inactivation of ShakerB K^+ channels. *Biophys. J.* 67:1806–1815.
Hackos, D.H., T.H. Chang, and K.J. Swartz. 2002. Scanning the intracellular s6 activation gate in the Shaker K^+ channel. *J. Gen. Physiol.* 119:521–532.
Heginbotham, L., and R. MacKinnon. 1993. Conduction properties of the cloned Shaker K^+ channel. *Biophys. J.* 65:2089–2096.
Holmgren, M., K.S. Shin, and G. Yellen. 1998. The activation gate of a voltage-gated K^+ channel can be trapped in the open state by an intersubunit metal bridge. *Neuron.* 21:617–621.
Holmgren, M., P.L. Smith, and G. Yellen. 1997. Trapping of organic blockers by closing of voltage-dependent K^+ channels: evidence for a trap door mechanism of activation gating. *J. Gen. Physiol.* 109:527–535.
Horn, R., S. Ding, and H.J. Gruber. 2000. Immobilizing the moving parts of voltage-gated ion channels. *J. Gen. Physiol.* 116:461–476.
Hoshi, T., W.N. Zagotta, and R.W. Aldrich. 1990. Biophysical and molecular mechanisms of Shaker potassium channel inactivation. *Science.* 250:533–538.
Hoshi, T., W.N. Zagotta, and R.W. Aldrich. 1994. Shaker potassium channel gating. I: Transitions near the open state. *J. Gen. Physiol.* 103:249–278.
Islas, L.D., and F.J. Sigworth. 1999. Voltage sensitivity and gating charge in Shaker and Shab family potassium channels. *J. Gen. Physiol.* 114:723–741.
Jiang, Y., A. Lee, J. Chen, M. Cadene, B.T. Chait, and R. MacKinnon. 2002a. Crystal structure and mechanism of a calcium-gated potassium channel. *Nature.* 417:515–522.
Jiang, Y., A. Lee, J. Chen, M. Cadene, B.T. Chait, and R. MacKinnon. 2002b. The open pore conformation of potassium channels. *Nature.* 417:523–526.
Jiang, Y., A. Lee, J. Chen, V. Ruta, M. Cadene, B.T. Chait, and R. MacKinnon. 2003. X-ray structure of a voltage-dependent K^+ channel. *Nature.* 423:33–41.
Kamb, A., J. Tseng-Crank, and M.A. Tanouye. 1988. Multiple products of the *Drosophila* Shaker gene may contribute to potassium channel diversity. *Neuron.* 1:421–430.
Kuo, A., J.M. Gulbis, J.F. Antcliff, T. Rahman, E.D. Lowe, J. Zimmer, J. Cuthbertson, F.M. Ashcroft, T. Ezaki, and D.A. Doyle. 2003. Crystal structure of the potassium channel KirBac1.1 in the closed state. *Science.* 300:1922–1926.
Ledwell, J.L., and R.W. Aldrich. 1999. Mutations in the S4 region isolate the final voltage-dependent cooperative step in potassium channel activation. *J. Gen. Physiol.* 113:389–414.
Li-Smerin, Y., D.H. Hackos, and K.J. Swartz. 2000a. Alpha-helical structural elements within the voltage-sensing domains of a K^+ channel. *J. Gen. Physiol.* 115:33–49.
Li-Smerin, Y., and K.J. Swartz. 1998. Gating modifier toxins reveal a conserved structural motif in voltage-gated Ca^{2+} and K^+ channels. *Proc. Natl. Acad. Sci. USA.* 95:8585–8589.
Li-Smerin, Y., and K.J. Swartz. 2000. Localization and molecular determinants of the hanatoxin receptors on the voltage-sensing domain of a K^+ channel. *J. Gen. Physiol.* 115:673–684.
Li-Smerin, Y., and K.J. Swartz. 2001. Helical structure of the COOH terminus of S3 and its contribution to the gating modifier toxin receptor in voltage-gated ion channels. *J. Gen. Physiol.* 117:205–218.
Liu, Y., M. Holmgren, M.E. Jurman, and G. Yellen. 1997. Gated access to the pore of a voltage-dependent K^+ channel. *Neuron.* 19: 175–184.
Lu, Z., A.M. Klem, and Y. Ramu. 2001. Ion conduction pore is conserved among potassium channels. *Nature.* 413:809–813.
Lu, Z., A.M. Klem, and Y. Ramu. 2002. Coupling between voltage sensors and activation gate in voltage-gated K^+ channels. *J. Gen. Physiol.* 120:663–676.
MacKinnon, R., R.W. Aldrich, and A.W. Lee. 1993. Functional stoichiometry of Shaker potassium channel inactivation. *Science.* 262: 757–759.
Mannuzzu, L.M., and E.Y. Isacoff. 2000. Independence and cooperativity in rearrangements of a potassium channel voltage sensor revealed by single subunit fluorescence. *J. Gen. Physiol.* 115:257–268.
Matteson, D.R., and R.P. Swenson, Jr. 1986. External monovalent cations that impede the closing of K^+ channels. *J. Gen. Physiol.* 87: 795–816.
Melishchuk, A., and C.M. Armstrong. 2001. Mechanism underlying slow kinetics of the OFF gating current in Shaker potassium channel. *Biophys. J.* 80:2167–2175.
Miller, C. 1995. The charybdotoxin family of K^+ channel-blocking peptides. *Neuron.* 15:5–10.
Murrell-Lagnado, R.D., and R.W. Aldrich. 1993a. Energetics of Shaker K channels block by inactivation peptides. *J. Gen. Physiol.* 102:977–1003.
Murrell-Lagnado, R.D., and R.W. Aldrich. 1993b. Interactions of amino terminal domains of Shaker K channels with a pore blocking site studied with synthetic peptides. *J. Gen. Physiol.* 102:949–975.
Roux, B., S. Berneche, and W. Im. 2000. Ion channels, permeation, and electrostatics: insight into the function of KcsA. *Biochemistry.* 39:13295–13306.
Schoppa, N.E., and F.J. Sigworth. 1998a. Activation of Shaker potassium channels. I. Characterization of voltage- dependent transitions. *J. Gen. Physiol.* 111:271–294.
Schoppa, N.E., and F.J. Sigworth. 1998b. Activation of Shaker potassium channels. II. Kinetics of the V2 mutant channel. *J. Gen. Physiol.* 111:295–311.
Schoppa, N.E., and F.J. Sigworth. 1998c. Activation of Shaker potassium channels. III. An activation gating model for wild-type and V2 mutant channels. *J. Gen. Physiol.* 111:313–342.
Smith-Maxwell, C.J., J.L. Ledwell, and R.W. Aldrich. 1998a. Role of the S4 in cooperativity of voltage-dependent potassium channel activation. *J. Gen. Physiol.* 111:399–420.
Smith-Maxwell, C.J., J.L. Ledwell, and R.W. Aldrich. 1998b. Uncharged S4 residues and cooperativity in voltage-dependent potassium channel activation. *J. Gen. Physiol.* 111:421–439.
Soler-Llavina, G.J., M. Holmgren, and K.J. Swartz. 2003. Defining the conductance of the closed state in a voltage-gated K^+ channel. *Neuron.* 38:61–67.

Swartz, K.J. 2001. Independent movement of voltage-sensing domains in the drk1 K^+ channel revealed by a gating modifier toxin. *Biophys. J.* 80:440a.

Swartz, K.J., and R. MacKinnon. 1997a. Hanatoxin modifies the gating of a voltage-dependent K^+ channel through multiple binding sites. *Neuron.* 18:665–673.

Swenson, R.P., Jr., and C.M. Armstrong. 1981. K^+ channels close more slowly in the presence of external K^+ and Rb^+. *Nature.* 291: 427–429.

Yellen, G. 1998. The moving parts of voltage-gated ion channels. *Q. Rev. Biophys.* 31:239–295.

Yifrach, O., and R. MacKinnon. 2002. Energetics of pore opening in a voltage-gated K^+ channel. *Cell.* 111:231–239.

Zagotta, W.N., and R.W. Aldrich. 1990. Voltage-dependent gating of Shaker A-type potassium channels in *Drosophila* muscle. *J. Gen. Physiol.* 95:29–60.

Zagotta, W.N., T. Hoshi, and R.W. Aldrich. 1990. Restoration of inactivation in mutants of Shaker potassium channels by a peptide derived from ShB. *Science.* 250:568–571.

Zagotta, W.N., T. Hoshi, and R.W. Aldrich. 1994a. Shaker potassium channel gating. III: Evaluation of kinetic models for activation. *J. Gen. Physiol.* 103:321–362.

Zagotta, W.N., T. Hoshi, J. Dittman, and R.W. Aldrich. 1994b. Shaker potassium channel gating. II: Transitions in the activation pathway. *J. Gen. Physiol.* 103:279–319.

Zheng, J., and F.J. Sigworth. 1997. Selectivity changes during activation of mutant Shaker potassium channels. *J. Gen. Physiol.* 110: 101–117.

Zheng, J., and F.J. Sigworth. 1998. Intermediate conductances during deactivation of heteromultimeric Shaker potassium channels. *J. Gen. Physiol.* 112:457–474.

Zhou, M., J.H. Morais-Cabral, S. Mann, and R. MacKinnon. 2001a. Potassium channel receptor site for the inactivation gate and quaternary amine inhibitors. *Nature.* 411:657–661.

Zhou, Y., J.H. Morais-Cabral, A. Kaufman, and R. MacKinnon. 2001b. Chemistry of ion coordination and hydration revealed by a K^+ channel-Fab complex at 2.0 Å resolution. *Nature.* 414: 43–48.